EasyChair Preprint

№ 4346

Backstepping Sliding Mode Control Strategy of Non-Contact 6-DOF Lorentz Force Platform

Quan Zhang and Qing Xiao

October 10, 2020

Backstepping sliding mode control strategy of non-contact 6-DOF Lorentz force platform

Quan Zhang
Shanghai University
Shanghai, China
lincolnquan@shu.edu.cn

Qing Xiao
Shanghai University
Shanghai, China
sharphepburn@shu.edu.cn

***Abstract*—With the development of aerospace technology, more and more scientific activities are carried out in the universe. Due to the microgravity environment of space, the force and control of the 6-DOF platform are completely different from those on the earth. Aiming at the 6-DOF non-contact platform in space microgravity environment, this paper built a virtual prototype model in ADAMS. The control-oriented dynamics equations were derived according to the model parameters. And the 6-DOF backstepping sliding mode controller and interference observer were designed in MATLAB/Simulink. Combining virtual prototype model and control system, the co-simulation model was proposed. According to the simulation results, the 6-DOF backstepping sliding mode controller can control the dynamic equation model or virtual prototype model within 0.5s effectively. And the correctness of the dynamic model is verified. In the simulation of applying sweep interference to the floating platform, it can be concluded that after 2s, the controller designed in this paper can control the displacement and angle of the floating platform within 2.5×10^{-6} m and 1.5×10^{-5} rad, which were lower than the traditional sliding mode controller by 90% and 78.6%, respectively. However, the input forces of biaxial non-contact Lorentz force drivers were within 1N, which is only 17.2% of the traditional sliding mode controller.**

Keywords: virtual prototype; backstepping sliding mode control; non-contact platform; interference observer; control-oriented;

I. INTRODUCTION

With the development of aerospace technology, scientific and technological activities under the space microgravity environment are increasing gradually. Micro-vibration has always been an dominant factor influencing space science experiment activities [1]. It widely exists in space microgravity environment and reduces the ideal working conditions for scientific and technological activities in space. High-frequency vibrations include crew activities on the spacecraft and air conditioning. Low-frequency vibration sources include solar panel tremor, gravity gradient resistance, and wind wheel imbalance. They are sufficient to reduce the performance of ultra -precision instruments, such as high-resolution cameras or remote laser communication [2].

For an optical observation lens, a vibration of 10 microns in space will cause an observation error of 500 km on the ground [3]. Therefore, the micro-vibration suppression and isolation technology on the spacecraft has received more and more attention from scholars [4].

Passive vibration isolation and active vibration isolation are two important forms of vibration isolation. However, passive vibration isolation technology is often powerless in the face of low-frequency vibration [5]. With the development of vibration isolation technology in recent years, active vibration isolation technology has made great progress in the microgravity environment. Active vibration isolation has a strong ability to attenuate low-frequency vibration in any environment [6].

In recent years, active vibration isolation platforms have achieved many new results. Currently, active vibration isolation platforms used in space microgravity environments are mainly divided into two categories, namely the traditional Stewart platform and the new drive platform. The Stewart platform belongs to a parallel robot structure [7]. In the same time, the related theoretical research and practical application are relatively mature. However, its response speed is slow relatively. New drive platforms such as piezoelectric vibration isolation platform and magnetic suspension vibration isolation platform [8]. Due to high accuracy and high response characteristics, piezoelectric actuators are widely used in positioning and vibration control [9]. Nevertheless, its displacement is only in the micron level, which is not suitable for millimeter-level micro vibration isolation. The Lorentz force driver mounted on the magnetic suspension vibration isolation platform has the characteristics of fast response speed and precise positioning ability. It is suitable for positioning and vibration isolation control of space-sensitive payloads.

There are several examples of control research on non-contact platforms. J.-l. LI, J.-b. WANG, and W. HE proposed a 6-DOF platform control transfer function model, using PID control to achieve vibration isolation and positioning control [10]. Q. Wu, H. Yue, R. Liu, L. Ding, and Z. Deng used eight single-axis Lorentz force actuators to achieve over-constraint control of the platform, and established a dynamic model including cables. In the meanwhile, compared PID control with sliding mode control [11].

In this paper, a virtual prototype of the non-contact 6-DOF platform is built in the ADAMS software. In the meantime, the 6-DOF backstepping sliding mode control algorithm with interference observer is studied [12]. The current work is organized as follows. In Section 2, the virtual prototype model

the National Natural Science Foundation of China under Grants of 61973207 and 51605271

Shanghai Rising-Star Program under Grant 20QA1403900, the Natural Science Foundation of Shanghai under Grant of 19ZR1474000

the State Key Laboratory of Mechanics and Control of Mechanical Structures （Nanjing University of Aeronautics and astronautics, Grant No. MCMS-E-0320G01）

is presented. The control-oriented Kane dynamics equations are derived in Section 3. Then in Section 4, 6-DOF backstepping sliding mode controller and interference observer are designed. Co-simulation model is built in Section 5. To verify the system's performance, simulations are carried out in Section 6. Finally, the conclusions are summarized in Section 7.

II. INTRODUCTION OF THE VIRTUAL PROTOTYPE MODEL

The 3D model of the platform was assembled through CREO, and then the virtual prototype was constructed in ADAMS software. As shown in Fig.1, the entire 6-DOF platform is deployed in a space-free environment. The floating platform and the fixed platform are connected by three biaxial non-contact Lorentz force actuators (Biaxial NLFA) [13]. The three actuators are separated by 120°. And each Biaxial NLFA can generates two driving forces, which are the force directed to the z-axis and a force along the tangential direction of the floating platform. The interference force application point can be set at any position of the floating platform, and it contains interference forces in three orthogonal directions.

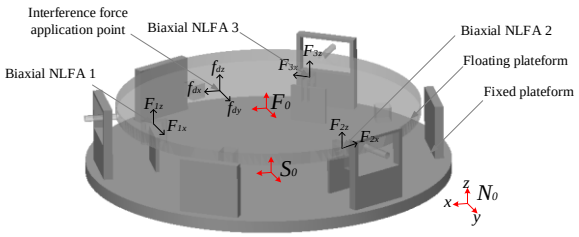

Fig.1 Non-contact 6-DOF platform virtual prototype

III. CONTROL-ORIENTED DYNAMICS

In Fig.1, where N_0 is the inertial coordinate system, S_0 is the fixed platform coordinate system, and F_0 is the floating platform coordinate system. Among them, the fixed platform is fixed together with the spacecraft, and there is only a small angle of rotation between S_0 and N_0, which can be ignored. And F_0 can be converted to S_0 through coordinate transformation matrix ${}^{(S/F)}C$.

In the case of small-angle rotation coordinate transformation, the transformation matrix can be simplified as:

$$ {}^{(S/F)}C = \begin{bmatrix} 1 & -\theta_z & \theta_y \\ \theta_z & 1 & -\theta_x \\ -\theta_y & \theta_x & 1 \end{bmatrix} \tag{1} $$

According to the Kane dynamic formula combined with the coordinate system transformation matrix, the dynamic equation of the floating platform can be derived as follows:

$$ \begin{bmatrix} F_{u1} \\ M_{u1} \end{bmatrix} + \begin{bmatrix} F_{v1} \\ M_{v1} \end{bmatrix} = \begin{bmatrix} m \cdot I_{3\times3} & 0 \\ 0_{3\times3} & {}^{(S/F)}C \cdot J_F \end{bmatrix} \ddot{X} \tag{2} $$

Where,

X is the vector of translation and rotation, which can be represented as:

$$ X = [x \quad y \quad z \quad \theta_x \quad \theta_y \quad \theta_z]^T $$

The vector of control force in x, y and z directions can be expressed as:

$$ F_{u1} = [F_x \quad F_y \quad F_z]^T $$

The vector of control torque around the x, y and z axis can be taken as:

$$ M_{u1} = [M_x \quad M_y \quad M_z]^T $$

Any interference force exerted on the floating platform can be resolved as a 6-DOF component around the center of mass of the floating platform, which can be expressed as:

$$ F_{v1} = \begin{bmatrix} F_{vx} & F_{vy} & F_{vz} \end{bmatrix}^T $$

$$ M_{v1} = \begin{bmatrix} M_{vx} & M_{vy} & M_{vz} \end{bmatrix} $$

The moment of inertia matrix of the floating platform can be marked as:

$$ J_F = \begin{bmatrix} J_{xx} & 0 & 0 \\ 0 & J_{yy} & 0 \\ 0 & 0 & J_{zz} \end{bmatrix} $$

The third-order identity matrix can be expressed as follows:

$$ I_{3\times3} = \begin{bmatrix} 1 & 0 & 0 \\ 0 & 1 & 0 \\ 0 & 0 & 1 \end{bmatrix} $$

In order to facilitate the design of the control algorithm, the dynamic formula can be represented as:

$$ F_u + F_v = M_x \ddot{X} \tag{3} $$

IV. DESIGN OF CONTROLLER AND SOLVER

In this paper, the backstepping sliding mode control and interference observer are combined and applied to the non-contact 6-DOF vibration isolation platform. The controller designed need to make the entire 6-DOF closed-loop system meet the expected dynamic and static performance indicators by comprehensively considering the control law and interference observations. And according to the position of the Biaxial NLFA, the input force solution matrix is derived.

A. Description of control system

The state space equation of the 6-DOF platform can be described as:

$$ \begin{aligned} \dot{x}_1 &= x_2 \\ \dot{x}_2 &= M_x^{-1} \cdot F_u + F_v \end{aligned} \tag{4} $$

Where, F_v is the total uncertainty, which can be predicted by the 6-DOF interference observer.

B. Design of backstepping sliding mode controller

Assuming that the Ideal position is x_d, the tracking error matrix can be expressed as:

$$z_1 = x_1 - x_d$$

Then,

$$\dot{z}_1 = x_2 - \dot{x}_d$$

Define the Lyapunov function:

$$V_1 = \frac{1}{2} z_1^{\,2} \tag{5}$$

Define x2:

$$x_2 = z_2 + \dot{x}_d - c_1 z_1$$

Where c_1 is a positive real number.

And z_2 is a virtual control item, which can be represented as:

$$z_2 = x_2 - \dot{x}_d + c_1 z_1$$

Therefore,

$$\dot{z}_1 = x_2 - \dot{x}_d = z_2 - c_1 z_1$$

$$\dot{V}_1 = z_1 \dot{z}_1 = z_1 z_2 - c_1 z_1^{\,2}$$

Define the switching function as:

$$\sigma = k_1 z_1 + z_2 \tag{6}$$

Where, $k_1>0$.

Since

$$\dot{z}_1 = z_2 - c_1 z_1$$

then

$$\sigma = k_1 z_1 + z_2 = k_1 z_1 + \dot{z}_1 + c_1 z_1$$

$$= (k_1 + c_1) z_1 + \dot{z}_1$$

Since $k_1+c_1>0$, obviously, if $\sigma=0$, then $z_1=0$, $z_2=0$ and $\dot{V}_1 \le 0$. For this, the next step of design is needed.

Define the Lyapunov function:

$$V_2 = V_1 + \frac{1}{2}\sigma^2 \tag{7}$$

then

$$\dot{V}_2 = V_1 + \sigma\dot{\sigma} = z_1 z_2 - c_1 z_1^{\,2} + \sigma\dot{\sigma}$$

$$= z_1 z_2 - c_1 z_1^{\,2} + \sigma(k_1(z_2 - c_1 z_1) + \dot{x}_2 - \ddot{x}_d + c_1 \dot{z}_1)$$

$$= z_1 z_2 - c_1 z_1^{\,2} + \sigma(k_1(z_2 - c_1 z_1) + M_x^{-1} F_u + F_v - \ddot{x}_d + c_1 \dot{z}_1)$$

The backstepping slide mode controller can be designed as:

$$F_u = M_x(-k_1(z_2 - c_1 z_1) + \ddot{x}_d - c_1 \dot{z}_1 - h(\sigma + \beta \operatorname{sgn}(\sigma))) - \hat{F}_v \tag{8}$$

Where, h and β are six-order diagonal matrices, and the elements on the diagonal are all positive real numbers. $\hat{F}_v$ is the observation vector of the interference observer.

Then

$$\dot{V}_2 = z_1 z_2 - c_1 z_1^{\,2} + \sigma(-h(\sigma + \beta \operatorname{sgn}(\sigma)) + F_v - \hat{F}_v)$$

$$\le z_1 z_2 - c_1 z_1^{\,2} - h\sigma^2 - h\beta |\sigma|$$

Take

$$N = \begin{bmatrix} c_1 + hk_1^{\,2} & hk_1 - \frac{1}{2} \\ hk_1 - \frac{1}{2} & h \end{bmatrix} \tag{9}$$

Because

$$z^T N z = \begin{bmatrix} z_1 & z_2 \end{bmatrix} \begin{bmatrix} c_1 + hk_1^{\,2} & hk_1 - \frac{1}{2} \\ hk_1 - \frac{1}{2} & h \end{bmatrix} \begin{bmatrix} z_1 & z_2 \end{bmatrix}^T$$

$$= c_1 z_1^{\,2} - z_1 z_2 + hk_1^{\,2} z_1^{\,2} + 2hk_1 z_1 z_2 + h z_2^{\,2} \tag{10}$$

$$= c_1 z_1^{\,2} - z_1 z_2 + h\sigma^2$$

where,

$$z = \begin{bmatrix} z_1 & z_2 \end{bmatrix}^T$$

Then if it is guaranteed that N is a positive definite matrix, we have

$$\dot{V}_2 \le -z^T N z - h\beta |\sigma| \le 0$$

Since

$$|N| = h(c_1 + k_1) - \frac{1}{4}$$

By selecting the values of h, c_1 and k_1, N can be made a positive definite matrix, thus ensuring $\dot{V}2 \le 0$. Therefore, the backstepping slide mode controller can achieve stable control.

C. Design of interference observer

The interference observer is designed as:

$$\dot{z} = -KF_u - K\hat{F}_v \tag{11}$$

$$\hat{F}_v = z + KM_x\dot{X} \tag{12}$$

where, $\hat{F}_v$ is the 6-DOF interference observation value vector of the floating platform. And K is taken as:

$$K=\begin{bmatrix} k_{11} & 0 & 0 & 0 & 0 & 0 \\ 0 & k_{22} & 0 & 0 & 0 & 0 \\ 0 & 0 & k_{33} & 0 & 0 & 0 \\ 0 & 0 & 0 & k_{44} & 0 & 0 \\ 0 & 0 & 0 & 0 & k_{55} & 0 \\ 0 & 0 & 0 & 0 & 0 & k_{66} \end{bmatrix}$$

D. Calculation of input force of Biaxial NLFA

According to Fig.1, it can be seen that the direction matrix of the input force of the Biaxial NLFA can be expressed under F_0 as:

$$\begin{bmatrix} P_{F1z}^T \\ P_{F1x}^T \\ P_{F2z}^T \\ P_{F2x}^T \\ P_{F3z}^T \\ P_{F3x}^T \end{bmatrix}=\begin{bmatrix} 0 & 0 & 1 \\ 0 & 1 & 0 \\ 0 & 0 & 1 \\ -\sqrt{3}/2 & -1/2 & 0 \\ 0 & 0 & 1 \\ \sqrt{3}/2 & -1/2 & 0 \end{bmatrix} \tag{13}$$

The position matrix of the three Biaxial NLFA can be expressed as follows under F_0:

$$\begin{bmatrix} R_{F_1}^T \\ R_{F_1}^T \\ R_{F_1}^T \end{bmatrix}=\begin{bmatrix} r_f & 0 & -d_v \\ -r_f/2 & \sqrt{3}r_f/2 & -d_v \\ -r_f/2 & -\sqrt{3}r_f/2 & -d_v \end{bmatrix} \tag{14}$$

According to the position of the three Biaxial NLFA on the floating platform and the coordinate transformation matrix, we can see:

$$F_u=\begin{bmatrix} {}^{(S/F)}CH_1 \\ {}^{(S/F)}CH_2 \end{bmatrix}F_{in} \tag{15}$$

where, the input force vector of the three Biaxial NLFA can be expressed as:

$$F_{in}=\begin{bmatrix} F_{1z} & F_{1x} & F_{2z} & F_{2x} & F_{3z} & F_{3x} \end{bmatrix}^T$$

The solution matrix can be taken as:

$$H_1=\begin{bmatrix} 0 & 0 & 0 & -\sqrt{3}/2 & 0 & \sqrt{3}/2 \\ 0 & 1 & 0 & -1/2 & 0 & -1/2 \\ 1 & 0 & 1 & 0 & 1 & 0 \end{bmatrix}$$

$$H_2^T=\begin{bmatrix} 0 & -r_f & 0 \\ d_v & 0 & r_f \\ \sqrt{3}r_f/2 & r_f/2 & 0 \\ -d_v/2 & \sqrt{3}d_v/2 & r_f \\ -\sqrt{3}r_f/2 & r_f/2 & 0 \\ -d_v/2 & -\sqrt{3}d_v/2 & r_f \end{bmatrix}$$

V. INTRODUCTION OF THE CO-SIMULATION MODEL

This paper used ADAMS software to complete the mechanical dynamics system modeling of the 6-DOF platform, and used MATLAB/Simulink to develop the 6-DOF control system program. The specific steps were to import the virtual prototype model in the ADAMS software into MATLAB/Simulink, and used S-function to write the programs of the backstepping sliding mode control module, the interference observer module and the dynamics module to realize the co-simulation. In Fig.2, the "Dynamics equations" module is generated according to the dynamic equations in Section 3. The "ADAMS_sub" module is a virtual prototype model derived from Adams software. The "Back-stepping sliding mode controller" module is a 6-DOF control model adapted from the control algorithm in Section 4. And the "Interference observer" module can observe the 6-DOF component of any interference force on the floating platform.

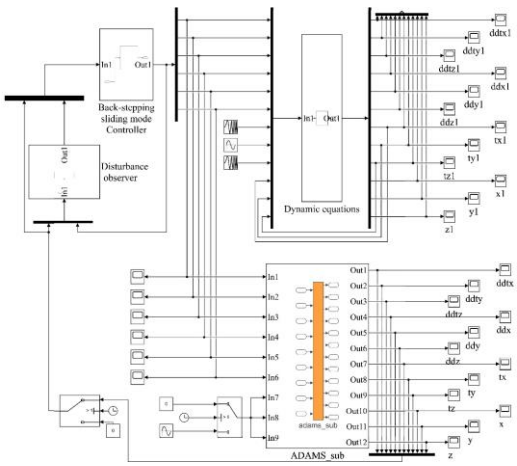

Fig.2 Combined model of dynamic system and control system

VI. MODEL VERIFICATION AND SIMULATION ANALYSIS

This section mainly verified the dynamic equations model and the virtual prototype model in ADAMS, and analyzed the simulation results.

A. Co-simulation model verification

To verify the correctness of the co-simulation model, it is necessary to verify that the 6-DOF control system is effective. The 6-DOF control system was designed based on Kane

dynamics equations. Therefore, it is essential to verify the consistency of the feedback of the control system through the "ADAMS_sub" module and the "Dynamic equations" module.

The control conditions were set as:

(1) The controller started control after interference was applied to the floating platform for 1 *s*.

(2) The interference input on the interference source was set as: x, y and z directions were sinusoidal interference with a magnitude of 1 *N* and a frequency of 50 *Hz*.

As shown in Fig.3 and Fig.4, in 0~1 *s* the floating platform is only affected by sinusoidal interference, and the backstepping sliding mode controller started to control the floating platform at 1*s*. The controller can realize stable control of the floating platform within 0.5 seconds. The degree of fit between the simulation trajectory of the "Dynamic equations" module and the simulation trajectory of the "ADAMS_sub" module can reach more than 98.5%. The results show the correctness of the derivation of the 6-DOF dynamic formula for the floating platform, and also show that the control program is reliable and has a certain degree of stability.

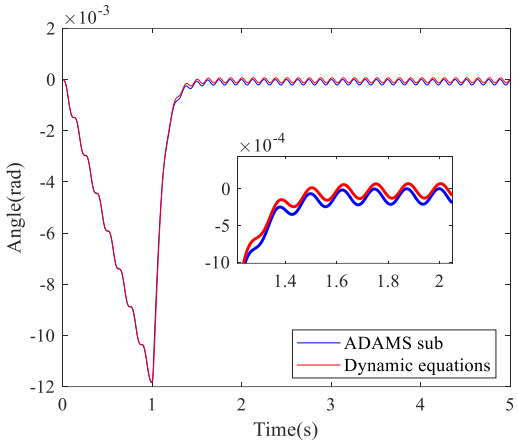

Fig.3 Virtual prototype verification (θ_y)

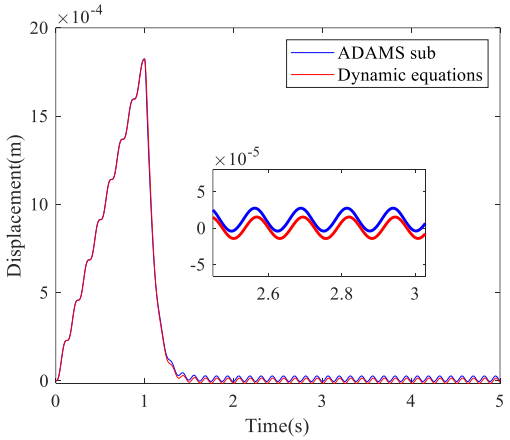

Fig.4 Virtual prototype verification (z)

B. Simulation analysis

The simulation conditions are set as follows: Sweep frequency interference with a frequency of 0.1-100 *Hz* and a magnitude of 1*N* was applied to the x, y, and z axes of the interference source within 0~5*s*.

As shown in Fig.5, the 6-DOF backstepping sliding mode controller (BSMC) designed in this paper can control the vibration amplitude within 1×10^{-5} *m* after 1 *s*, and the displacement trajectory shows a trend of convergence. Otherwise, the traditional sliding mode controller (SMC) has no obvious trend of convergence in suppressing the amplitude. And in 3.6 ~ 4 *s*, it can be observed that the position control of the floating platform using BSMC is 90% more accurate than that of SMC.

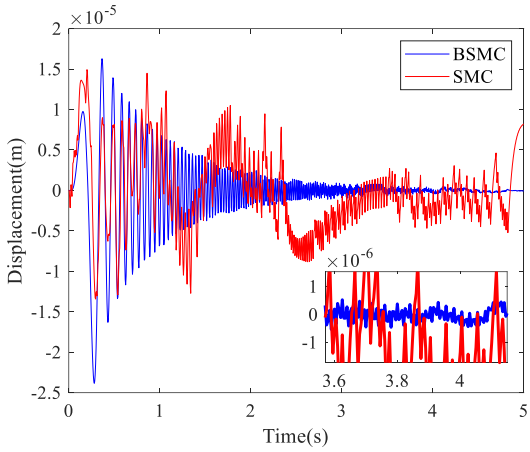

Fig.5 Comparison of displacement control effects (*z*)

In Fig.6, it can be seen that the performance of BSMC for angle control is better than SMC. And after 2 *s*, BSMC can control the angle of rotation of the floating platform around the z axis within 1.5×10^{-5} *rad*. On the contrary, SMC can only control the angle around 7×10^{-5} *rad*.

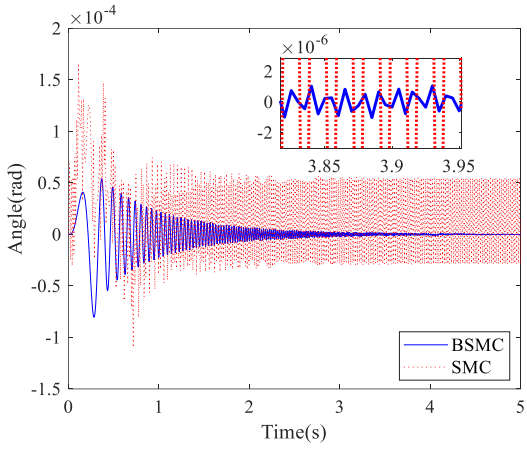

Fig.6 Comparison of angle control effects(θ_z)

It can be concluded from Fig.7 that peak value of the input force of Biaxial NLFA 1 in the z direction is below 1*N* when BSMC is used. In contrast, the peak value of input force is around 5.8 *N* when using SMC.

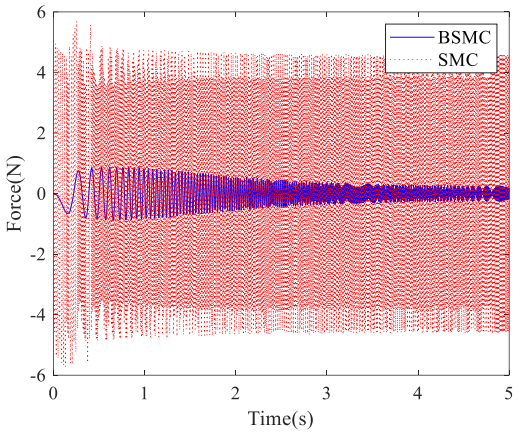

Fig7. Input force of Biaxial NLFA 1 (F_{1z})

The performance of BSMC was analyzed under the condition of applying sweep frequency interference to the floating platform. The simulation results show that after 2*s*, the amplitudes of position and angle control of the floating platform by the BSMC are 90% and 78.6% lower than that of the SMC respectively. On the contrary, the input force required of Biaxial NLFA 1 in the z direction is only 17.2% of SMC.

VII. CONCLUSION

Based on the virtual prototype model parameters established in ADAMS software, this paper derived the 6-DOF dynamics equations under the space microgravity environment. A 6-DOF backstepping sliding mode controller(BSMC) is designed and equipped with a 6-DOF interference observer. Based on the position of Biaxial NLFA on the platform, the input force solution matrix is derived. According to the design of the controller, a control program is designed in MATAB/Simulink. In the co-simulation of the dynamic system and the control system, the model was verified, and the results showed that the degree of fit between the dynamic formula model and the virtual prototype model was above 98.5%. In the simulation of applying sweep frequency interference to the floating platform, it can be concluded that after 2 *s*, the 6-DOF BSMC controlled the amplitude of position and angle of the floating platform by 90% and 78.6%, respectively. And its input force required was only 17.2% of SMC.

ACKNOWLEDGMENT

Q.X thanks the National Natural Science Foundation of China under Grants of 61973207 and 51605271, Shanghai Rising-Star Program under Grant 20QA1403900, the Natural Science Foundation of Shanghai under Grant of 19ZR1474000, and the State Key Laboratory of Mechanics and Control of Mechanical Structures （Nanjing University of Aeronautics and astronautics, Grant No. MCMS-E-0320G01）

REFERENCES

[1] Z. Gong et al., "System integration and control design of a maglev platform for space vibration isolation," Journal of Vibration and Control, vol. 25, no. 11, pp. 1720-1736, 2019.

[2] L. Li, L. Tan, L. Kong, D. Wang, and H. Yang, "The influence of flywheel micro vibration on space camera and vibration suppression," Mechanical Systems and Signal Processing, vol. 100, pp. 360-370, 2018.

[3] T. D. Le and K. K. Ahn, "Active pneumatic vibration isolation system using negative stiffness structures for a vehicle seat," Journal of Sound Vibration, vol. 333, no. 5, pp. 1245-1268, 2014.

[4] C. Liu, X. Jing, S. Daley, and F. Li, "Recent advances in micro-vibration isolation," Mechanical Systems and Signal Processing, vol. 56, pp. 55-80, 2015.

[5] C. Hansen, S. Snyder, X. Qiu, L. Brooks, and D. Moreau, Active control of noise and vibration. CRC press, 2012.

[6] C. Wang, Y. Chen, and Z. Zhang, "Simulation and experiment on the performance of a passive/active micro-vibration isolator," Journal of Vibration and Control, vol. 24, no. 3, pp. 453-465, 2018.

[7] C. Wang, X. Xie, Y. Chen, and Z. Zhang, "Investigation on active vibration isolation of a Stewart platform with piezoelectric actuators," Journal of Sound and Vibration, vol. 383, pp. 1-19, 2016.

[8] F. Yang et al., "A Novel 2-DOF Lorentz Force Actuator for the Modular Magnetic Suspension Platform," Sensors, vol. 20, no. 16, p. 4365, 2020.

[9] E. Arshid and A. R. Khorshidvand, "Free vibration analysis of saturated porous FG circular plates integrated with piezoelectric actuators via differential quadrature method," Thin-Walled Structures, vol. 125, pp. 220-233, 2018.

[10] J.-l. LI, J.-b. WANG, and W. HE, "Electromechanical co-simulation analysis for contactless positioning and vibration isolation platform," Journal of ZheJiang University (Engineering Science), vol. 53, no. 1, pp. 146-157, 2019.

[11] Q. Wu, H. Yue, R. Liu, L. Ding, and Z. Deng, "Simulation of multi-closed loop control with feed forward control of micro-vibration isolation platform," in ASME 2014 International Mechanical Engineering Congress and Exposition, 2014, pp. V04AT04A006-V04AT04A006: American Society of Mechanical Engineers.

[12] J. Liu, Sliding mode control using MATLAB. Academic Press, 2017.

[13] J. Li and W. He, "Modeling and Analysis of a Biaxial Noncontact Lorentz Force Actuator," IEEE Transactions on Magnetics, vol. 55, no. 4, pp. 1-9, 2019.